

Molecular Mechanisms that Govern the Specificity of Sushi Peptides for Gram-Negative Bacterial Membrane Lipids[†]

Peng Li,[‡] Miao Sun,[‡] Thorsten Wohland,[§] Daiwen Yang,[‡] Bow Ho,^{||,⊥} and Jeak Ling Ding^{*,‡,⊥}

Departments of Biological Sciences, Chemistry, and Microbiology, National University of Singapore, Singapore

Received February 9, 2006; Revised Manuscript Received June 19, 2006

ABSTRACT: Factor C-derived Sushi peptides (S1 and S3) have been shown to bind lipopolysaccharide (LPS) and inhibit the growth of Gram-negative bacteria but do not affect mammalian cells. On the premise that the composition of membrane phospholipids differs between the microbial and human cells, we studied the modes of interaction between S1 and S3 and the bacterial membrane phospholipids, POPG, in comparison to that with the mammalian cell membrane phospholipids, POPC and POPE. S1 exhibits specificity against POPG, suggesting its preference for bacterial anionic phospholipids, regardless of whether the phospholipids form vesicles in a solution or a monolayer on a solid surface. The specificity of the Sushi peptides for POPG is a consequence of the electrostatic and hydrophobic forces. The unsaturated nature of POPG confers fluidity to the lipid layer, and being in the proximity of LPS in the microenvironmental milieu, POPG probably enhances the insertion of the peptide–LPS complex into the bacterial inner membrane. Furthermore, during its interaction with POPG, the S1 peptide underwent a transition from random to α -helical coil, while S3 became a mixture of β -sheet and α -helical structures. This differential structural change in the peptides could be responsible for their different modes of disruption of POPG vesicles. Conceivably, the selectivity for POPG spares the mammalian membranes from undesirable effects of antimicrobial peptides, which could be helpful in designing and developing a new generation of antibiotics and in offering some clues about the specific function of Factor C, a LPS biosensor.

Gram-negative bacteria (GNB)¹ are among the most challenging pathogens to the human host (1–3). Sushi peptides have been demonstrated to bind and kill an opportunistic Gram-negative bacterium, *Pseudomonas aeruginosa* (4), while exhibiting minimal cytotoxicity to human monocytes, THP-1 (5). However, the molecular mechanisms that govern the specificity of the Sushi peptides for Gram-negative bacterial membranes are not well defined. Previous reports have focused on the effects of these peptides on LPS.

It has been shown that S1 recognizes and binds LPS with high affinity (5). However, among the LPS molecules on the outer membrane of Gram-negative bacteria are phospholipids, which are also localized on the inner membrane (6). This prompted us to investigate the interaction between S1 and phospholipids. Phospholipids are important constituents of both the bacterial and mammalian cell membranes, but the composition of phospholipids on the membrane of bacteria is rather different from that of mammalian cells (7). The mammalian cell membrane comprises mainly phosphatidylcholine (~45% PC), phosphatidylethanolamine (~15% PE), phosphatidylserine (~5% PS), and small amounts of other phospholipids, most of which are neutral at physiological pH. In contrast, bacterial membranes such as that of *Pseudomonas* (8) harbor substantial amounts of negatively charged phospholipids, such as phosphatidylglycerol (PG), besides neutral phospholipids, PE (Figure 1A).

Although previous reports investigated the interaction of bacterial phospholipids and other peptides, they are limited to the headgroups of bacterial phospholipids (9–11). In this work, we investigated not only the effects of the headgroups and the lipid tails but also the effect of the unsaturated nature of POPG on their interaction with LPS-binding peptides, Sushi (S1 and S3). We examined the detailed molecular mechanisms underlying the contribution of the membrane phospholipids to the specificity of the peptides, particularly S1. Wherever relevant, comparisons were made with S3. Our results demonstrate that the electrostatic force between S1 and the anionic headgroup of POPG plays the key role in the specificity of interaction. Nevertheless, hydrophobic

[†] We thank the BMRC, Agency for Science Technology and Research (A* STAR), Singapore, for funding support. P.L. is a recipient of a Research Scholarship from the National University of Singapore. M.S. is an undergraduate scholar of the National University of Singapore, in receipt of the Singapore Government Undergraduate Scholarship for Flow-through Pre-U Chinese Scholars.

* To whom correspondence should be addressed: Department of Biological Sciences, National University of Singapore, 14, Science Dr. 4, Singapore 117543. Telephone: (65) 6874-2776. Fax: (65) 6779-2486. E-mail: dbsdjl@nus.edu.sg.

[‡] Department of Biological Sciences.

[§] Department of Chemistry.

^{||} Department of Microbiology.

[⊥] Co-senior authors.

¹ Abbreviations: CD, circular dichroism; DPPG, dipalmitoylphosphatidylglycerol; FCS, fluorescence correlation spectroscopy; GNB, Gram-negative bacteria; HPA, hydrophobic affinity sensor chip; LPS, lipopolysaccharide; PC, phosphatidylcholine; PE, phosphatidylethanolamine; PG, phosphatidylglycerol; POPC, palmitoyloleoylphosphatidylcholine; POPE, palmitoyloleoylphosphatidylethanolamine; POPG, palmitoyloleoylphosphatidylglycerol; POPS, palmitoyloleoylphosphatidylserine; PVDF, polyvinylidene fluoride; REV, rhodamine-entrapped vesicles; RLV, rhodamine-labeled vesicles; S1, Sushi 1 peptide; S3, Sushi 3 peptide; SPR, surface plasmon resonance; τ_{DL} , diffusion time of the large particle; TMR, tetramethylrhodamine.

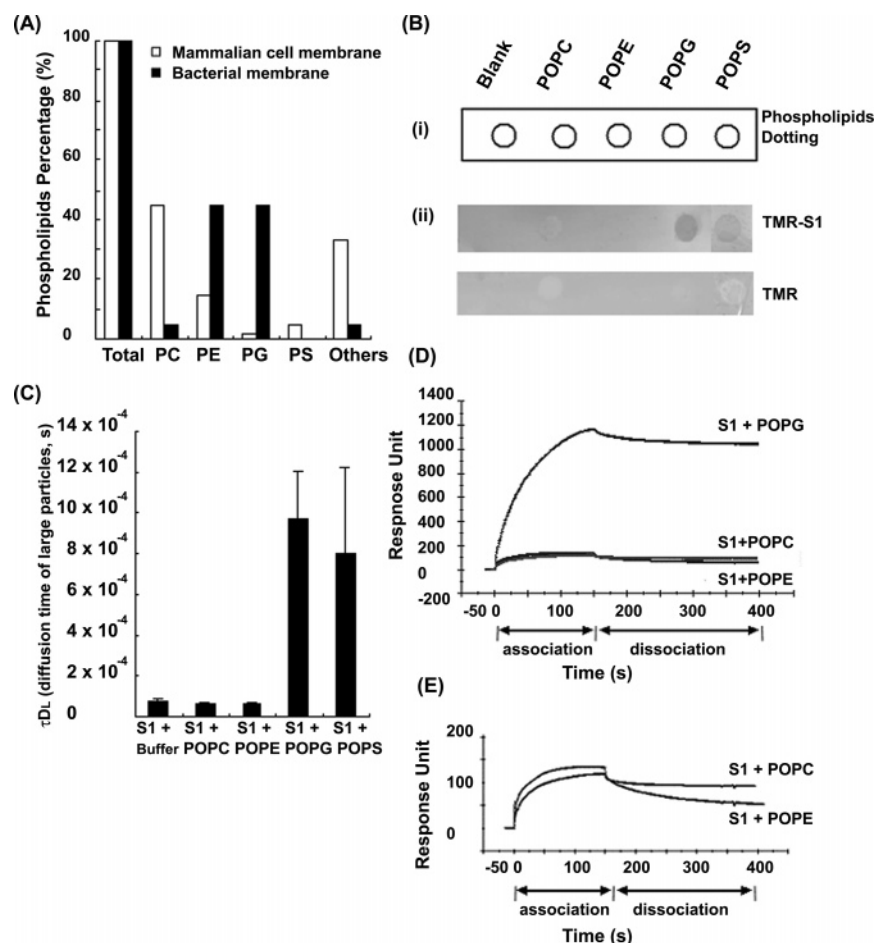


FIGURE 1: S1 specifically binds POPG and not POPC or POPE. (A) The composition of phospholipids on membranes. White bars are for the mammalian cell membrane, and black bars for the bacterial (*Pseudomonas*) membrane. This plot is based on information obtained from refs 9 and 43. (B) A peptide–phospholipid dot blot assay was carried out with the PVDF membrane strips spotted with phospholipids. (i) Aliquots (5 μ L) of different phospholipids (POPC, POPE, POPG, and POPS) were dotted on the membrane. (ii) Specific interaction is observed between TMR-S1 and POPG and POPS. The lack of interaction between TMR and the phospholipids further confirms the specificity of interaction between TMR-S1 and POPG. (C) Determination of the τ_{DL} (the diffusion time of large particles in seconds) of TMR-S1 in different solutions of phospholipids shows that TMR-S1 interacts with POPG. The control was phosphate buffer. (D) Sensorgrams depicting the real-time biointeraction between the S1 peptides and the immobilized phospholipids (POPC, POPE, and POPG). The real-time biointeraction analysis at a flow rate of 20 μ L/min also indicates the preference of S1 for POPG. (E) Enlargement of the sensorgrams of POPC and POPE, depicting the real-time biointeraction between the S1 peptides and the immobilized phospholipids (POPC and POPE).

interaction contributes a significant driving force of interaction between antimicrobial peptides and GNB, and it is generally thought that the lipid tails on the GNB membrane offer a strong hydrophobic environment (12, 13). However, the lipid tails of phospholipids from bacterial and mammalian membranes share similarity. Thus, we investigated the hydrophobic interaction between S1 and different phospholipids and show that hydrophobic interaction occurred between the peptide and the lipid tails of POPG only but not with other zwitterionic phospholipids. Besides this, considering the dynamism of the biologically functional membrane, which can be attributed to the unsaturated nature of the phospholipids (14), we compared the unsaturated POPG with its saturated counterpart, DPPG, to address the influence of unsaturation on the interaction with S1. This observation was confirmed with a temperature assay. To this end, we employed various approaches using different forms of the phospholipids (both in solution and immobilized on a solid surface) to provide more detailed evidence for the mechanism of interaction between the S1 peptides and phospholipids. Our data demonstrate that POPG is responsible for the specificity of the Sushi peptides for bacteria

and that both the electrostatic and hydrophobic interactions contribute significantly to this specific binding. The propensity for transitions in the secondary structures unique to each of these peptides in the presence of POPG probably explains their selectivity for the bacterial membranes. Since S1 and S3 peptides are derived from two different LPS-binding domains of the Factor C molecule (5), it explains why Factor C is such a highly sensitive and specific biosensor for anionic lipids of Gram-negative bacteria.

MATERIALS AND METHODS

Peptide Synthesis and Materials. Peptides used in this study were synthesized and purified by Genemed Synthesis Inc. (San Francisco, CA). The S1 peptide (N-GFKLKG-MARISCLPNGQWSNFPKCIKRECAMVSS-C), with a molecular mass of 3758 Da, corresponds to residues 171–204 of the Sushi 1 domain of horseshoe crab Factor C (GenBank accession number S77063). The S3 peptide (N-HAEH-KVKIGVEQKYQGFPQGTETVYTCSGNYFLM-C), with a molecular mass of 3892 Da, corresponds to residues 268–301 of the Factor C Sushi 3 domain. TMR-S1 is S1 labeled at the N-terminus with a fluorescent probe, TMR (tetra-

methyrlhodamine). All peptides were purified by high-performance liquid chromatography to >95% purity. Phospholipids (POPC, POPE, POPG, and POPS) were purchased from Avanti (St. Louis, MO). Pyrogen-free water for making buffers was from Baxter (Morton Grove, IL).

Preparation of Phospholipid Vesicles. The vesicles were prepared by mixing the phospholipids in a 9:3:1 POPC:POPE:POPS ratio and a 1:1 POPE:POPG ratio. Briefly, dry lipids were dissolved in chloroform. The solvent was evaporated under a stream of nitrogen, and the lipids were held under vacuum. The phospholipids were then resuspended in 20 mM phosphate buffer by vortex mixing. The resultant dispersed lipid, at a concentration of 0.5 mM with respect to phospholipids, was then sonicated and extruded through a 50 nm polycarbonate filter to obtain homogeneity in the size of vesicles (44–46).

To understand the effect of the peptides on POPG vesicles, two differently labeled POPG vesicles were further prepared: rhodamine-entrapped vesicles (REV) and rhodamine-labeled vesicles (RLV). Unlabeled POPG was used to prepare vesicles. REV were constructed by addition of free rhodamine 6G during vesicle preparation. Since rhodamine-PG is not commercially available, for studies with RLV, rhodamine-PE was mixed with POPG in a ratio of 1:19 by the extrusion technique. Prior to extrusion, a dried lipid film was dispersed by vortex mixing in buffer containing rhodamine 6G and rhodamine-PE. REV and RLV were purified from unincorporated rhodamine 6G and rhodamine-PE by chromatography through microSpin S-200 HR columns (Pharmacia Biotech, Uppsala, Sweden) which removed free rhodamine 6G and rhodamine-PE. REV and RLV were stored at 4 °C (15).

Dot Blotting. To determine the specificity of binding of peptides to the phospholipids-on-matrix, a PVDF membrane was first dotted with 5 μ L of each of the phospholipids. The phospholipid dots were evaporated, and the membrane was washed three times with water before blocking with a wash solution containing 3% BSA at room temperature for 3 h (16). After two washings, the fluorescently labeled peptide (TMR-S1) and control (TMR) were allowed to interact with the phospholipid dots at room temperature for 3 h. Peptides that were bound to the immobilized phospholipids were detected by red fluorescence.

Surface Plasmon Resonance. The interactions between the peptides and phospholipids on the solid phase were studied by surface plasmon resonance (SPR), where the phospholipids (POPE, POPC, POPG, and DPPG) coated on a HPA chip could presumably mimic the biological membrane. The real-time interaction between different concentrations of peptides and phospholipids was performed according to the method of Tan et al. (5), using a BIAcore 2000 instrument (Pharmacia). The SPR was recorded on the phospholipid-coated HPA chip blocked with skim milk. The HPA chip was regenerated by a pulse of 0.1 N NaOH until the SPR reached baseline. The spectra were baseline-corrected by subtraction of blank spectra of the corresponding solutions without peptide. The temperature within the sample chamber was maintained at 25 or 37 °C.

Circular Dichroism. The secondary structure transformation of 5 μ M peptides induced by 100 μ M phospholipids was monitored by CD. CD spectra were recorded in 20 mM phosphate buffer (pH 7.0) using a Jasco-J-810 CD spectropolarimeter. The spectra were recorded in quartz cell

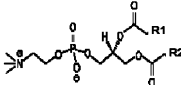
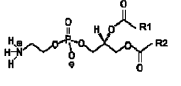
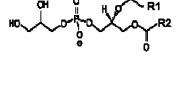
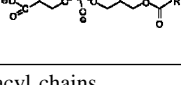
cuvettes with a path length of 10 mm. The following parameters were used: bandwidth of 2 nm, step resolution of 0.5 nm, response of 1 s, scan speed of 10 nm/min, and scan width of 190–260 nm. The temperature within the sample chamber was maintained at 25 °C with a continuous flow of nitrogen. Calibration was carried out with D-camphorsulfonic acid.

Trp Fluorescence Scanning Spectroscopy and Fluorescence Quenching Assay. To investigate the potential hydrophobic interaction between peptide and phospholipids, we measured the fluorescence change due to the tryptophan (Trp) residue in S1 (17). The fluorescence scanning spectra were obtained with a spectrofluorimeter (Perkin-Elmer, LS 50B) by using an excitation wavelength of 280 nm, and the emission was scanned from 290 to 450 nm at a rate of 10 nm/s. Each spectrum was the average of 10 scans. The spectra were baseline-corrected by subtracting blank spectra of the corresponding solutions without peptide. All samples contained 5 μ M peptide in 20 mM phosphate buffer (pH 7.0), and the concentration of phospholipids was 100 μ M. For fluorescence quenching experiments, acrylamide was added from a 4 M stock solution to final concentrations between 0.05 and 0.5 M. The quenched samples were excited at 280 nm, and the emission was monitored at the peak maximum determined from the wavelength scan in the absence of quencher. The effect of the acrylamide on the fluorescence of the peptide was analyzed using the F_i/F_0 ratio, where F_i is the fluorescence peak intensity of Trp with arylamide and F_0 is the fluorescence peak intensity without arylamide (18).

Fluorescence Correlation Spectroscopy. The FCS instrument is a self-built system that is centered around a Zeiss Axiovert 200 inverted microscope using an excitation source and an argon–krypton laser which has a 530 nm line for TMR excitation. The dichroic and emission filters (Omega Optical, Brattleboro, VT) were 570DRLP and 595AF60 filters for TMR, respectively. Further details on the FCS setup and theory are described by Wohland et al. (19) and Krichinsky et al. (20), respectively. FCS measurements were conducted at a constant concentration of 50 nM TMR-S1 with different phospholipid vesicles at 5 μ M. The sample solutions were prepared at least 2 h before the measurements to ensure that binding equilibrium had been reached. A 50 μ L droplet of the corresponding sample was then placed on a cover slip just before the measurement. The background signal in water and in the corresponding buffers was less than 0.2 kHz. All measurements were precalibrated with TMR and TMR-S1 to ensure the proper performance of the instrument (21). For each sample, at least 10 independent measurements were recorded, and the mean reading was calculated.

We examined the interaction between the Sushi peptides and the vesicles (REV and RLV) in solution by FCS. The diffusion time of REV and RLV was monitored using FCS. The measurements were conducted at different concentrations of peptide and 1 μ M phospholipid vesicles. The anticipated possibilities are as follows. (i) If the vesicles remain intact, the diffusion time (τ_{DL}) of REV and RLV will not change. (ii) If the peptide disrupts the vesicles, the free rhodamine and rhodamine-PE will be released from REV and RLV, respectively; thus, the τ_{DL} of REV and RLV will decrease. (iii) The peptide forms channels only on the surface of

Table 1: Characteristics of Four Kinds of Phospholipids^a

Phospholipid	Full-name	Chemical structure*	Head group	Source
PC	phosphatidylcholine		zwitterionic	Mammalian cell membrane
PE	Phosphatidylethanolamine		zwitterionic	Mammalian cell/bacterial membrane
PG	Phosphatidylglycerol		anionic	Bacterial membrane
PS	Phosphatidylserine		anionic	Mammalian cell membrane

^a R1 and R2 are fatty acyl chains.

vesicles, causing the τ_{DL} of REV to decrease because the entrapped rhodamine in the center of the REV will be released through the channels, while the τ_{DL} of RLV will remain unchanged. This is because the rhodamine-PE is only labeled on the surface of RLV. With the help of the fluorescently labeled REV and RLV, we can clearly monitor the peptide-mediated effects on the vesicles in solution (15).

RESULTS

S1 Specifically Binds Anionic POPG and Not Zwitterionic POPC and POPE. Here, we used a dot blotting approach to examine whether S1 peptide can differentiate the phospholipids from bacteria and mammalian cell membranes. Figure 1B shows that TMR-S1 specifically binds to anionic POPG and POPS and not the zwitterionic phospholipids, POPC and POPE. These binding assays indicate that the dissimilarity in specificity was probably attributable to the charge difference among POPC, POPE, POPG, and POPS (Table 1). Consistent with dot blotting results, the FCS analysis showed that TMR-S1 has a stronger affinity for anionic POPG and POPS than for zwitterionic POPC and POPE in solution (Figure 1C). At the initial stage, TMR-S1 exists in a free form as the predominant fluorescent species. During the course of the interaction, τ_{DL} increased, demonstrating that the percentage of the complex between TMR-S1 and phospholipid increased as the small fluorescently labeled peptide binds the large unlabeled phospholipid vesicles.

To mimic the phospholipid layer of the biomembrane, we coated the phospholipids on a biacore chip activated with a hydrophobic surface. Real-time interaction analysis measured as a surface plasmon resonance, SPR, of the binding between S1 and various phospholipids was carried out. A set of sensorgrams of S1 interacting with different phospholipids was used to demonstrate the affinity (Figure 1D). The increasing association curves describe the initial binding of the peptide to the phospholipids immobilized on the HPA chip, and the decreasing curves relate to the dissociation in real time. This trend was consistently observed for the binding of peptides to pure vesicles containing 100% POPC, POPE, or POPG. The sensorgrams revealed that the SPR signal intensity measured in response units (RU) increased as a function of the concentration of the peptide bound to

the immobilized phospholipids. This indicates that the amount of peptide bound to the lipid is related to the affinity of the peptide for the phospholipids-on-chip. This is consistent with the dot blot result (Figure 1B), which clearly demonstrates that S1 binds more strongly to the anionic POPG than to the two zwitterionic phospholipids, POPC and POPE.

Hydrophobic Interaction Contributes Significantly to the Binding Specificity of S1 to POPG. We use Trp fluorescence scanning spectroscopy to study the hydrophobic interaction between S1 and phospholipids. The penetration of S1 into the phospholipid vesicles was confirmed by determining the fluorescence emission spectra due to the Trp residue in S1 when in the presence of the phospholipids. The addition of anionic phospholipids, 100% POPG, 100% POPS, or a 1:1 POPE/POPG mixture to the peptide sample caused a blue shift of 4 nm in the emission peak, from 354 to 350 nm (Figure 2A,B). This blue shift indicates that the Trp residue was partitioned into a more hydrophobic environment, which would be expected if the Trp residue was positioned among the acyl chains of the phospholipid. In POPG, the fluorescence intensity increased, suggesting that the Trp residue was more sterically confined. In contrast, when the zwitterionic lipids, POPC/POPE/POPS mixture, POPC, or POPE, were reacted with S1, there was no blue shift (Figure 2A,B), indicating that the local environment of Trp was kept in an original state as there was no interaction between S1 and zwitterionic lipids.

To determine the extent to which S1 was sequestered in the hydrophobic core of the vesicle, a fluorescence quenching experiment was performed using acrylamide. This study was based on the premise that the hydrophobic core residue, Trp, in S1 is involved in hydrophobic interactions with the phospholipids and that the fluorescence intensity of Trp is protected by phospholipids from acrylamide quenching. F/F_0 was calculated from the plots between 0 and 0.5 M acrylamide. In 0.2 M acrylamide, F/F_0 was 25.7% for S1, while in the presence of POPG, F/F_0 increased to 44.4%. In the presence of a POPE/POPG mixture, F/F_0 was 37.1% (Table 2). These values confirm that when the peptide is free in solution, it is much more accessible to the quencher (acrylamide) than in the presence of the anionic POPG vesicles. Since the phospholipids protect the Trp residues from the water-soluble acrylamide, it confirms that the S1 peptide was partially buried in the hydrophobic core of the vesicles.

Conformational change to the peptides could occur because of their hydrophobic interaction with the phospholipid vesicles. Therefore, we used CD measurements to examine the secondary structure of these peptides. In aqueous solution, S1 adopts a random coil conformation as shown by the single minimum at 200 nm (Figure 2C). With vesicles constructed using 100% POPC, POPE, POPG, or POPS, we observed that only the POPG and POPS vesicles can induce a conformational change in S1 (Figure 2C). In the presence of a mixture of anionic phospholipids (1:1 POPE/POPG), the S1 peptide exhibited a spectrum of characteristics of an α -helix, which presented as a pair of minima at 208 and 225 nm (Figure 2D). This is consistent with the CD spectrum of magainin (11). Furthermore, since the mammalian cell plasma membrane also contains ~5% anionic phospholipid, POPS (8, 43), we investigated the interaction between POPS

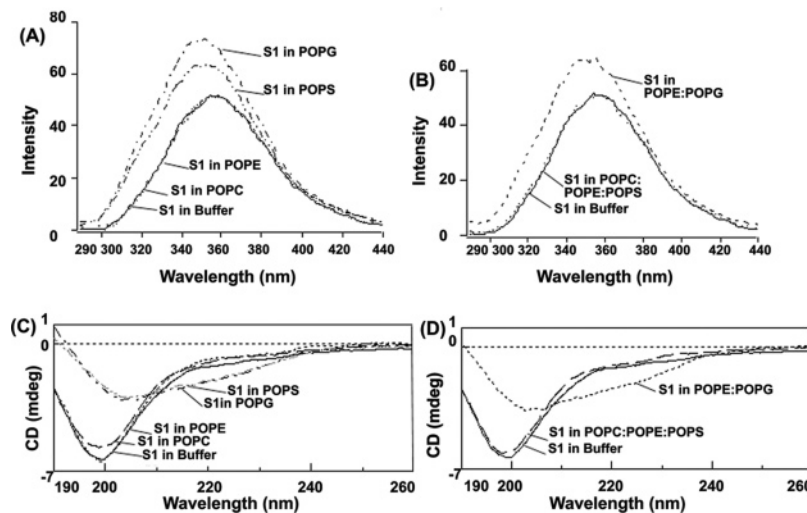


FIGURE 2: Hydrophobic interaction confers binding specificity of S1 peptide for POPG. (A) Trp fluorescence scanning spectroscopy shows the excitation fluorescence spectrum of S1 in individual phospholipids. (B) Trp fluorescence scanning spectroscopy of S1 in representative combinations of POPE and POPG (according to bacterial membrane phospholipid composition) and POPC, POPE, and POPS (according to mammalian membrane phospholipid composition). The blue shift in the presence of POPG indicates that the environment of Trp in S1 has been altered from a hydrophilic to a hydrophobic state. (C) CD spectra of S1 peptide in the presence of individual phospholipid solutions. (D) CD spectra of S1 in POPC/POPE/POPS and POPE/POPG solutions.

Table 2: F_i/F_0 Values^a Determined from Trp Fluorescence Quenching Experiments

[acrylamide] (M)	F_i/F_0 (%) (S1 in water)	F_i/F_0 (%) (S1 in POPG)	F_i/F_0 (%) (S1 in POPE and POPG)
0	100 ± 3.0	100 ± 1.6	100 ± 2.6
0.05	78.5 ± 3.2	80.3 ± 1.7	73.7 ± 2.6
0.1	56.3 ± 3.0	65.1 ± 1.0	56.9 ± 1.4
0.2	25.7 ± 1.5	44.4 ± 1.7	37.1 ± 1.0
0.5	5.60 ± 0.4	15.5 ± 1.6	12.1 ± 1.1

^a F_i is the fluorescence peak intensity of Trp with acrylamide and F_0 the fluorescence peak intensity without acrylamide.

and S1 peptide. Dot blotting results suggest that S1 exhibits a similar specificity for POPS, since the headgroup of POPS is also anionic (Figure 1B). CD spectrum indicates a conformational shift in the presence of POPS (Figure 2C), similar to that of POPG. Additionally, there was hydrophobic interaction between S1 and POPS (Figure 2A). However, in the presence of a mixture of mammalian membrane phospholipids (9:3:1 POPC/POPE/POPS), the S1 peptide exhibited no conformational change, which is unlike the bacterial membrane phospholipid mimic, a 1:1 POPE/POPG mixture (Figure 2D). Therefore, the peptide has little effect on the mixture of mammalian membrane phospholipids (Figure 2D). Taken together, the results suggest that the contribution of POPS to the mammalian cell membrane is insignificant, and the effect of anionic mammalian phospholipids on the peptide is minimal.

The Unsaturated Nature of POPG Enhances Its Interaction with S1. So far, we have demonstrated that both the headgroup and lipid tails of POPG are indispensable for the interaction with S1 peptide. Incidentally, POPG is unsaturated, and the fluidity of biological membranes can be attributed to its unsaturation. Thus, we compared the interactions between S1 peptide and the unsaturated POPG with the saturated DPPG. Comparatively, the intensity of Trp-mediated fluorescence change was higher in POPG than in DPPG (Figure 3A). Furthermore, S1 was more readily transformed into an α -helix in the presence of POPG rather than in DPPG (Figure 3B). The results suggest that S1 more

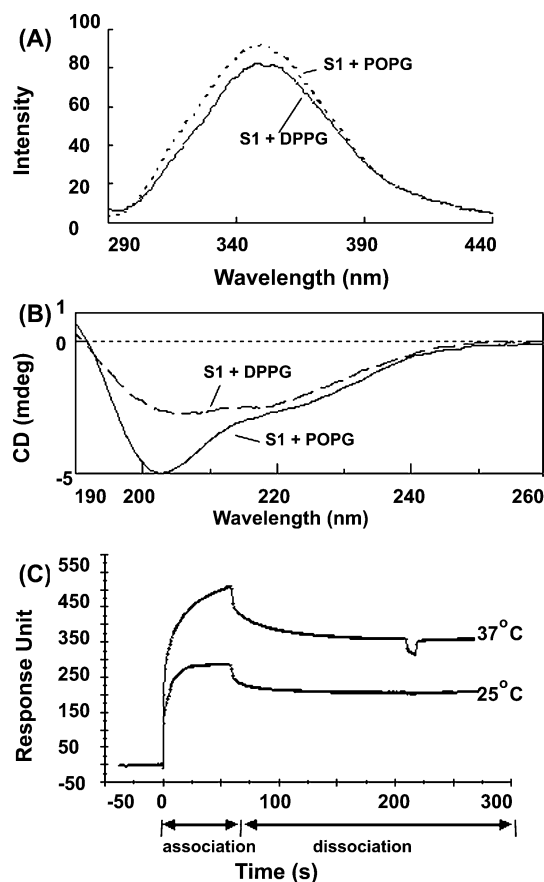


FIGURE 3: Effect of the unsaturated state of POPG on the interaction with S1 peptide. (A) Trp fluorescence scanning spectroscopy shows the excitation fluorescence spectrum of S1 in individual phospholipids, POPG or DPPG. (B) CD spectra of S1 peptide in the presence of individual phospholipid solutions. (C) Sensorgrams depicting the real-time biointeraction between the immobilized POPG and S1 at 25 and 37 °C, at a flow rate of 100 μ L/min.

easily inserts into the lipid tail of POPG than that of DPPG. Being unsaturated, POPG confers greater fluidity to the bacterial membrane. Furthermore, since temperature also affects the fluidity of a lipid layer, we monitored the real-

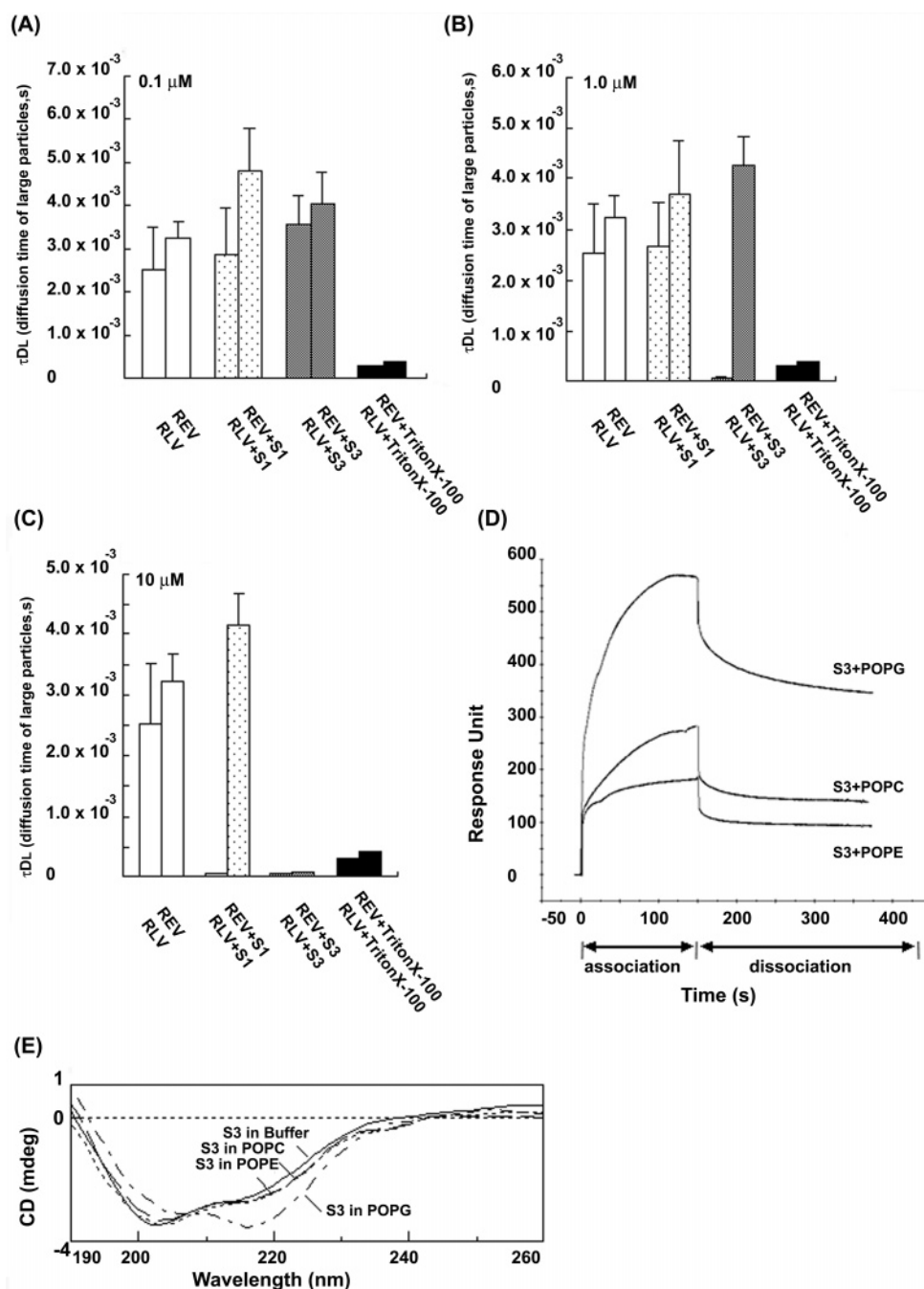


FIGURE 4: S1 and S3 show different modes of disruption of POPG vesicles. (A–C) Determination of the stoichiometry of interaction between POPG REV and Sushi peptides, τ_{DL} , the diffusion time of large particles (seconds). RLV were incubated with different concentrations of Sushi peptides: (A) 0.1, (B) 1, and (C) 10 μ M. As an internal positive control, Triton X-100 was used to disrupt the phospholipid vesicles. (D) Sensorgrams depicting the real-time biointeraction between the immobilized phospholipids and the S3 peptides using a flow rate of 20 μ L/min. (E) CD spectra of S3 peptide in the presence of individual phospholipid solutions.

time interaction between S1 and POPG at different temperatures (Figure 3C). The results showed that S1 binds more strongly at 37 $^{\circ}$ C than at 25 $^{\circ}$ C, suggesting that the unsaturated nature of POPG confers fluidity to the lipid layer and enhances the penetration of S1 into the bacterial membrane.

Sushi Peptides Disrupt POPG Vesicles. To date, the most popular hypotheses for the perturbation of the bacterial membrane by cationic antimicrobial peptides focus on the “carpet” and “barrel-stave” mechanisms (22, 23). To clarify the effect of perturbation induced by the Sushi peptides, we constructed two kinds of labeled POPG vesicles, REV and RLV, to interact with different concentrations of the peptides.

When REV and RLV were incubated with 0.1 and 1 μ M S1, the τ_{DL} did not decrease (Figure 4A,B), suggesting that the vesicles remained intact. It appears that S3 binds more readily to POPG so that at 1 μ M, it caused leakage to the vesicles. In contrast, it requires 10 μ M S1 to cause the same degree of leakage (Figure 4C) as 1 μ M S3, whereas at 10 μ M, S3 was causing total disruption, demonstrating that indeed, S3 disrupts POPG vesicles completely and more effectively at lower concentrations.

In comparison, S3 also exhibited a consistent preference for POPG (Figure 4D). However, unlike S1 and magainin (11) which are random in an aqueous environment (Figure 2C), S3 exhibited a mixture of α -helix, β -strand, and random

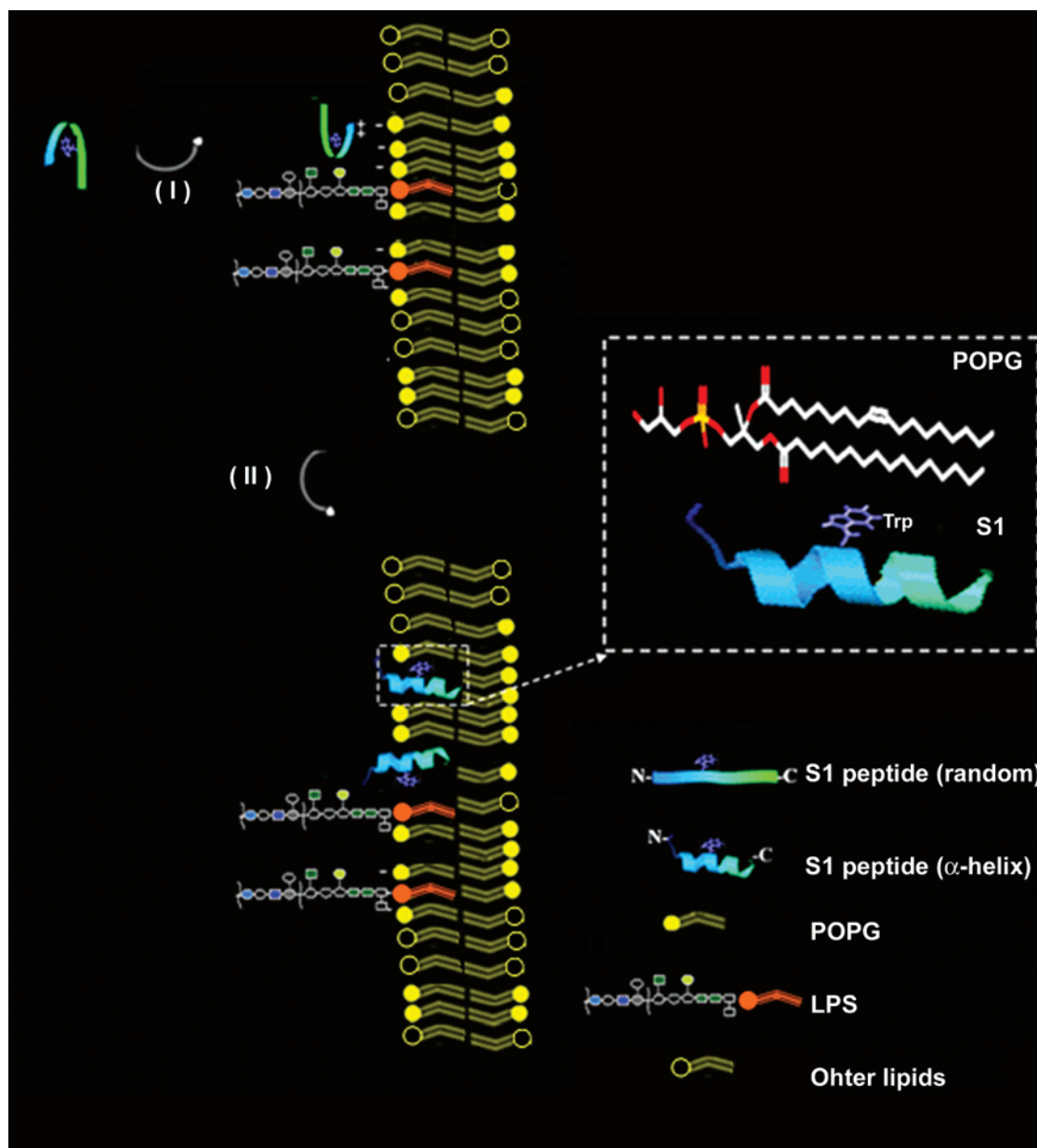


FIGURE 5: Molecular mechanism underlying the selective interaction between S1 and the POPG layer. S1 peptide specifically binds POPG via (I) electrostatic interactions between the positively charged amino acid residues near its N-terminus and the negatively charged bisphosphate headgroups of the POPG and (II) hydrophobic interactions between the hydrophobic region of S1 and the acyl chains of POPG. S1 forms an α -helical structure to insert into the POPG layer; thus, the Trp residue is probably protected by the lipid tail of POPG. The N-terminal region of S1 is colored blue, and C-terminus is colored green. Trp is colored lilac.

coil (Figure 4E). S3 remained unchanged in POPC and POPE, but the content of α -helicity increased slightly in the presence of POPG, giving a mixture of α -helix and β -sheet structures. Thus, the different manner of interaction between S1 and POPG and between S3 and POPG may be due to the different inherent secondary structures of the peptides induced by POPG itself.

DISCUSSION

While the mammalian cell membrane is composed mostly of neutral phospholipids, PC and PE, the *Pseudomonas* outer membrane is anionic, being rich in negatively charged PG. S1 peptides have been demonstrated to exhibit exceptional activity against *P. aeruginosa*, with minimal cytotoxicity to human monocytes (4, 5). Thus, we designed experiments to investigate the contribution of the phospholipid composition

to the specificity and selectivity of the S1 peptides for the *Pseudomonas* membrane. In this work, we used POPC and POPE to construct the mammalian cell membrane and POPG to simulate the bacterial membrane (24, 25). Since it has been reported that membrane phospholipids such as POPC and POPG can form unilamellar vesicles, while POPE forms hexagonal vesicles (26), we employed various biochemical and biophysical methods using different forms of the phospholipids (both in solution and on a solid surface) to provide compelling evidence for the mechanism of interaction between the peptides and the phospholipids (27).

By a series of analyses, we demonstrate that S1 and S3 peptides interact more strongly with anionic POPG than zwitterionic POPC and POPE. These results suggest that the phospholipid composition of biological membranes plays a crucial role in influencing and specifying the selectivity of

the peptide. The headgroup of POPG confers anionicity to it, whereas POPE and POPC are zwitterionic (Table 1). Mammalian cell plasma membranes contain ~5% anionic phospholipids, POPS (8, 43). Our results indicate that S1 exhibits a similar specificity for POPS, since the headgroup of POPS is also anionic, but the 9:3:1 POPC/POPE/POPS mixture of mammalian membrane phospholipids has little effect on the peptide (Figure 2B,D). This electrostatic difference between the phospholipids accounts partly for the charge difference between the mammalian and the Gram-negative bacterial cell membranes, ultimately contributing to the specificity of the antimicrobial peptides, which preferentially bind to the exposed anionic surface of bacterial membranes, but not to the zwitterionic amphiphiles present in the extracellular monolayer of mammalian plasma membranes. This could spare the mammalian host cells from any undesired peptide-induced injury. Thus, the initial electrostatic interaction determines the specificity of the S1 peptides for the bacterial membrane. Charge–charge interactions between the cationic peptides and the anionic phospholipids at the bacterial outer membrane are deemed to be the most critical binding force, explaining why the increase in the net positive charge of the peptides could enhance its binding to anionic lipids (28, 29). This is in agreement with our previous report that mutations of the N-terminus to introduce two extra lysine residues into S1 peptides resulted in an increase in LPS neutralizing activity (5). In concordance, these results suggest that the charge interaction is responsible for the selective binding between the peptides and the bacterial anionic phospholipids. On the other hand, the charge interaction is minimal with the mammalian cell membrane phospholipids (Figures 2), hence, its lack of cytotoxicity to the mammalian host.

Hydrophobic interaction contributes significantly to the binding force between the peptides and bacterial lipids (30, 31, 33). The Trp fluorescence scanning spectroscopy experiment revealed that the microenvironment of the S1 peptide was transformed from a hydrophilic to a more hydrophobic state, thus engaging the hydrophobic region of the peptide in an interactive bond with the acyl chains of the bacterial membrane phospholipids (32, 34), particularly that of anionic POPG. Other studies on cationic peptides, using NMR, Raman, and fluorescence measurements, have indicated that initially, an antimicrobial peptide would bind parallel to the lipid layer (35, 36). Because of the simultaneous electrostatic and hydrophobic interactions, the binding of Sushi peptides with anionic lipids is highly salt tolerant (37). In a high-salt environment, when the electrostatic interaction is weakened, the hydrophobic interaction is the major force that maintains the affinity of the S1 peptides for the anionic lipids. This study confirms that hydrophobic interaction between S1 and POPG is indispensable.

Our new data show that the unsaturated state of the lipid tail of POPG probably enhances the interaction between the peptide and POPG (Figure 3), which suggests that the unsaturated nature of the bacterial phospholipid confers fluidity to the membrane and possibly augments the insertion of such a peptide into the bacterial membrane (38). This finding was supported by a differential temperature assay of the real-time binding of S1 to POPG, which showed that at 37 °C where the unsaturated membrane environment is expected to be more fluidic than at 25 °C, S1 binds more

readily to the LPS. This observation should be taken into consideration and exploited for future design and development of novel antimicrobial drug peptides, to facilitate greater specificity of the peptides for the bacterial anionic unsaturated membrane lipids.

Previously, we have shown that S3 breaks the LPS layer (21). Our current work demonstrates that S1 and S3 disrupt the POPG vesicles. However, S1 and S3 elicit different degrees of disruption of POPG vesicles at the same dosage (Figure 4A–C). This difference appears to be consistent with the different secondary structures of the S1 and S3 peptides. While S1 is random in solution and becomes helical in an anionic lipid environment, S3 persistently exhibits more helical structure even in the absence of an anionic lipid (Figure 4E). Thus, although the phospholipid composition in the cell membrane may be the ultimate determinant of the binding specificity of a peptide, the structural propensity of the peptides in the microenvironment of the bacterial or mammalian membranes could strongly influence the structure and function of the molecule, which in turn determines its specificity for the lipids in the microenvironment. Because S1 and S3 peptides are derived from different LPS-binding domains of the Factor C molecule, it would appear that Factor C harbors rather versatile modes of interaction with bacterial lipids (39), where the α -helical and β -sheet structures of the Sushi domains may conceivably bind LPS and even cooperate to strengthen Factor C protein as an extremely sensitive biosensor to Gram-negative infection (40–42).

Here, we propose a model for the specific interaction between one of the Sushi peptides, S1, and POPG (Figure 5). Because of the negative charge on the headgroup of POPG and the positive charge that can be attributed to the Lys and Arg residues on the S1 peptide, specific charge–charge interaction occurs between S1 and membrane phospholipids during which the peptide is drawn close to the surface of the POPG layer (Figures 2–4). While being inserted into the microenvironment of the anionic phospholipids, S1 undergoes a change in conformation from random to α -helix. Thus, their positively charged amino acids face the negatively charged headgroups of the phospholipids, and their hydrophobic amino acids, such as Trp, insert into the lipid acyl chains (Figure 5).

REFERENCES

1. Zasloff, M. (2002) Antimicrobial peptides of multicellular organisms, *Nature* 415, 389–95.
2. Boneca, I. G. (2005) The role of peptidoglycan in pathogenesis, *Curr. Opin. Microbiol.* 8, 46–53.
3. Breithaupt, H. (1999) The new antibiotics, *Nat. Biotechnol.* 17, 1165–9.
4. Yau, Y. H., Ho, B., Tan, N. S., Ng, M. L., and Ding, J. L. (2001) High therapeutic index of factor C Sushi peptides: Potent antimicrobials against *Pseudomonas aeruginosa*, *Antimicrob. Agents Chemother.* 45, 2820–5.
5. Tan, N. S., Ng, M. L., Yau, Y. H., Chong, P. K., Ho, B., and Ding, J. L. (2000) Definition of endotoxin binding sites in horseshoe crab factor C recombinant sushi proteins and neutralization of endotoxin by sushi peptides, *FASEB J.* 14, 1801–13.
6. Lysko, P. G., and Morse, S. A. (1981) *Neisseria gonorrhoeae* cell envelope: Permeability to hydrophobic molecules, *J. Bacteriol.* 145, 946–52.
7. Hashimoto, M., Asai, Y., and Ogawa, T. (2003) Treponemal phospholipids inhibit innate immune responses induced by pathogen-associated molecular patterns, *J. Biol. Chem.* 278, 44205–13.

8. Graham, J., and Higgins, J. (1997) *Membrane analysis*, Springer, New York.
9. Blazys, J., Wiegand, R., Klein, J., Hammer, J., Epand, R. M., Epand, R. F., Maloy, W. L., and Kari, U. P. (2001) A novel linear amphipathic β -sheet cationic antimicrobial peptide with enhanced selectivity for bacterial lipids, *J. Biol. Chem.* 276, 27899–906.
10. Papo, N., and Shai, Y. (2003) Exploring peptide membrane interaction using surface plasmon resonance: Differentiation between pore formation versus membrane disruption by lytic peptides, *Biochemistry* 42, 458–66.
11. Tachi, T., Epand, R. F., Epand, R. M., and Matsuzaki, K. (2002) Position-dependent hydrophobicity of the antimicrobial magainin peptide affects the mode of peptide-lipid interactions and selective toxicity, *Biochemistry* 41, 10723–31.
12. Kondejewski, L. H., Jelokhani-Niaraki, M., Farmer, S. W., Lix, B., Kay, C. M., Sykes, B. D., Hancock, R. E., and Hodges, R. S. (1999) Dissociation of antimicrobial and hemolytic activities in cyclic peptide diastereomers by systematic alterations in amphipathicity, *J. Biol. Chem.* 274, 13181–92.
13. Biggin, P. C., and Sansom, M. S. (1999) Interactions of α -helices with lipid bilayers: A review of simulation studies, *Biophys. Chem.* 76, 161–83.
14. Saiz, L., and Klein, M. L. (2001) Influence of highly polyunsaturated lipid acyl chains of biomembranes on the NMR order parameters, *J. Am. Chem. Soc.* 123, 7381–7.
15. Pramanik, A., Thyberg, P., and Rigler, R. (2000) Molecular interactions of peptides with phospholipid vesicle membranes as studied by fluorescence correlation spectroscopy, *Chem. Phys. Lipids* 104, 35–47.
16. Hanada, K., Kumagai, K., Yasuda, S., Miura, Y., Kawano, M., Fukasawa, M., and Nishijima, M. (2003) Molecular machinery for non-vesicular trafficking of ceramide, *Nature* 426, 803–9.
17. Zhao, H., and Kinnunen, P. K. (2002) Binding of the antimicrobial peptide temporin L to liposomes assessed by Trp fluorescence, *J. Biol. Chem.* 277, 25170–7.
18. Eftink, M. R., and Ghiron, C. A. (1976) Exposure of tryptophanyl residues in proteins. Quantitative determination by fluorescence quenching studies, *Biochemistry* 15, 672–80.
19. Wohland, T., Rigler, R., and Vogel, H. (2001) The standard deviation in fluorescence correlation spectroscopy, *Biophys. J.* 80, 2987–99.
20. Krichinsky, O., and Bonnet, G. (2002) Fluorescence correlation spectroscopy: The technique and its applications, *Rep. Prog. Phys.* 65, 251–97.
21. Li, P., Wohland, T., Ho, B., and Ding, J. L. (2004) Perturbation of lipopolysaccharide (LPS) micelles by Sushi 3 (S3) antimicrobial peptide. The importance of an intermolecular disulfide bond in S3 dimer for binding, disruption, and neutralization of LPS, *J. Biol. Chem.* 279, 50150–6.
22. Oren, Z., Hong, J., and Shai, Y. (1997) A repertoire of novel antibacterial diastereomeric peptides with selective cytolytic activity, *J. Biol. Chem.* 272, 14643–9.
23. Epand, R. M., and Vogel, H. J. (1999) Diversity of antimicrobial peptides and their mechanisms of action, *Biochim. Biophys. Acta* 1462, 11–28.
24. Fernandez, C., Hilty, C., Wider, G., and Wuthrich, K. (2002) Lipid–protein interactions in DHPC micelles containing the integral membrane protein OmpX investigated by NMR spectroscopy, *Proc. Natl. Acad. Sci. U.S.A.* 99, 13533–7.
25. Mani, R., Buffy, J. J., Waring, A. J., Lehrer, R. I., and Hong, M. (2004) Solid-state NMR investigation of the selective disruption of lipid membranes by protegrin-1, *Biochemistry* 43, 13839–48.
26. McIntosh, T. J. (1996) Hydration properties of lamellar and non-lamellar phases of phosphatidylcholine and phosphatidylethanolamine, *Chem. Phys. Lipids* 81, 117–31.
27. Murzyn, K., Rog, T., and Pasenkiewicz-Gierula, M. (2005) Phosphatidylethanolamine-phosphatidylglycerol bilayer as a model of the inner bacterial membrane, *Biophys. J.* 88, 1091–103.
28. Tam, J. P., Lu, Y. A., and Yang, J. L. (2002) Correlations of cationic charges with salt sensitivity and microbial specificity of cystine-stabilized β -strand antimicrobial peptides, *J. Biol. Chem.* 277, 50450–6.
29. Hong, S. Y., Park, T. G., and Lee, K. H. (2001) The effect of charge increase on the specificity and activity of a short antimicrobial peptide, *Peptides* 22, 1669–74.
30. Frece, V., Ho, B., and Ding, J. L. (2000) Molecular dynamics study on lipid A from *Escherichia coli*: Insights into its mechanism of biological action, *Biochim. Biophys. Acta* 1466, 87–104.
31. Frece, V., Ho, B., and Ding, J. L. (2000) Interpretation of biological activity data of bacterial endotoxins by simple molecular models of mechanism of action, *Eur. J. Biochem.* 267, 837–52.
32. Brandenburg, K., David, A., Howe, J., Koch, M. H., Andra, J., and Garidel, P. (2005) Temperature dependence of the binding of endotoxins to the polycationic peptides polymyxin B and its nonapeptide, *Biophys. J.* 88, 1845–58.
33. Farnaud, S., Spiller, C., Moriarty, L. C., Patel, A., Gant, V., Odell, E. W., and Evans, R. W. (2004) Interactions of lactoferricin-derived peptides with LPS and antimicrobial activity, *FEMS Microbiol. Lett.* 233, 193–9.
34. Zhang, L., Scott, M. G., Yan, H., Mayer, L. D., and Hancock, R. E. (2000) Interaction of polyphemus I and structural analogs with bacterial membranes, lipopolysaccharide, and lipid monolayers, *Biochemistry* 39, 14504–14.
35. Bechinger, B., Zasloff, M., and Opella, S. J. (1998) Structure and dynamics of the antibiotic peptide PGLa in membranes by solution and solid-state nuclear magnetic resonance spectroscopy, *Biophys. J.* 74, 981–7.
36. Matsuzaki, K., Murase, O., Tokuda, H., Funakoshi, S., Fujii, N., and Miyajima, K. (1994) Orientational and aggregational states of magainin 2 in phospholipid bilayers, *Biochemistry* 33, 3342–9.
37. Ding, J. L., Zhu, Y., and Ho, B. (2001) High-performance affinity capture-removal of bacterial pyrogen from solutions, *J. Chromatogr., B: Biomed. Sci. Appl.* 759, 237–46.
38. Pande, A. H., Qin, S., and Tatulian, S. A. (2005) Membrane fluidity is a key modulator of membrane binding, insertion, and activity of 5-lipoxygenase, *Biophys. J.* 88, 4084–94.
39. Nakamura, T., Tokunaga, F., Morita, T., Iwanaga, S., Kusumoto, S., Shiba, T., Kobayashi, T., and Inoue, K. (1988) Intracellular serine-protease zymogen, factor C, from horseshoe crab hemocytes. Its activation by synthetic lipid A analogues and acidic phospholipids, *Eur. J. Biochem.* 176, 89–94.
40. Muta, T., and Iwanaga, S. (1996) The role of hemolymph coagulation in innate immunity, *Curr. Opin. Immunol.* 8, 41–7.
41. Ding, J. L., and Ho, B. (2001) A new era in pyrogen testing, *Trends Biotechnol.* 19, 277–81.
42. Ariki, S., Koori, K., Osaki, T., Motoyama, K., Inamori, K., and Kawabata, S. (2004) A serine protease zymogen functions as a pattern-recognition receptor for lipopolysaccharides, *Proc. Natl. Acad. Sci. U.S.A.* 101, 953–8.
43. Hauser, H., and Poupart, G. (1992) *The structure of biological membranes*, CRC Press, London.
44. Mayer, L. D., Hope, M. J., and Cullis, P. R. (1986) Vesicles of variable sizes produced by a rapid extrusion procedure, *Biochim. Biophys. Acta* 858, 161–8.
45. Carrozzino, J. M., Fuguet, E., Helburn, R., and Khaledi, M. G. (2004) Characterization of small unilamellar vesicles using solvatochromic π^* indicators and particle sizing, *J. Biochem. Biophys. Methods* 60, 97–115.
46. Korgel, B. A., van Zanten, J. H., and Monbouquette, H. G. (1998) Vesicle size distributions measured by flow field-flow fractionation coupled with multiangle light scattering, *Biophys. J.* 74, 3264–72.

BI0602765